phys. stat. sol. (a) 44, 325 (1977)

Subject classification: 1.1 and 18.3; 5; 22.8.2

*Institute of Physics, Jagiellonian University, Cracow*[1]) *(a), Boris Kidrič Institute, Vinča*[2]) *(b), and Institute of Physics, Silesian University, Katowice (c)*

# Investigations of Crystal and Magnetic Properties of Nickel Ferrite-Aluminates

By

J. J. BARA (a), A. T. PĘDZIWIATR (a), Z. M. STADNIK (a), A. SZYTUŁA (a), J. TODOROVIČ (b), Z. TOMKOWICZ (a), and W. ZAREK (c)

The crystal and magnetic properties of nickel ferrite-aluminates are investigated with X-ray, neutron diffraction, magnetometric, and Mössbauer effect methods. Variation of the saturation magnetic moment per molecule measured at 78 K with chemical composition is satisfactorily explained on the basis of the collinear spin ordering model and the elaborated and experimentally verified cation distributions model.

Es werden die Kristalleigenschaften und die magnetischen Eigenschaften von Aluminium-Nickel-Ferriten mit Hilfe von Röntgenstrahluntersuchungen, Neutronenbeugung, magnetometrischen Methoden und dem Mößbauereffekt untersucht. Die Änderung des magnetischen Sättigungsmomentes eines Moleküls mit der Änderung der chemischen Zusammensetzung, gemessen bei 78 K, wird auf der Grundlage des Modells der kollinearen Anordnung der Spines sowie des erarbeiteten und experimentell überprüften Modells befriedigend erklärt.

## 1. Introduction

Nickel ferrite-aluminates $NiFe_{2-t}Al_tO_4$ belong to a large class of compounds having the general formula $X^{2+}Y_2^{3+}O_4$ and crystallizing in a spinel structure. The parameter $t$ may be varied from zero to two, which covers the entire range from nickel ferrite $NiFe_2O_4$ to nickel aluminate $NiAl_2O_4$. The metal ions are situated in the oxygen tetrahedra (A-sites) and octahedra (B-sites). Nickel ferrite is an inverted spinel, i.e. all its $Ni^{2+}$ ions are located in B-sites. The same is thought to be true for nickel ferrite-aluminates with $0 < t < 0.9$. When $t$ varies from about 0.9 to 2.0 the $Ni^{2+}$ ions start to occupy the A-sites also [1]. In nickel aluminate the ratio of the $Al^{3+}$ ions in the A- and B-sites is about 2:3. Thus nickel ferrite-aluminates with $0.9 < t < 2.0$ and nickel aluminate are partially inverted spinels.

The crystal and magnetic properties of nickel ferrite-aluminates have been the subject of many investigations performed with different methods [2 to 6]. The basic magnetic properties of these materials depend on what kind of metal ions is present at the different sites and how these ions are distributed [2, 5, 6]. The ionic distributions have been observed to depend on a previous heat treatment of a sample. The antiferromagnetic A–B superexchange interaction is the main cause of the cooperative behaviour of the magnetic dipole moments, known as ferrimagnetism, which is observed in nickel ferrite-aluminates below their Curie temperatures. The A–B coupling is considerably stronger than that between the ions located in the same type of crystallographic site. The magnetic moments of the ions in octahedral positions are coupled parallel to one another and at the same time are antiparallel to the magnetic moments of the tetrahedral ions.

---

[1]) Reymonta 4, 30-059 Cracow, Poland.

[2]) Vinča, Yugoslavia.

In nickel ferrite the $Fe^{3+}$ ions are in the S-state. They show little deviation from the pure spin behaviour and have in principle the same magnetic moment values ($5\mu_B$) in A- and B-sites. Thus the measured value of the saturation magnetic moment per molecule $2.3\mu_B$ is determined solely by the magnetic moment of the divalent nickel ion. In nickel ferrite-aluminates the value of that moment is reduced by the non-magnetic $Al^{3+}$ ions.

The purpose of this paper is to present the results of investigations of the crystal and magnetic properties of nickel ferrite-aluminates obtained with X-ray, neutron diffraction, magnetometric, and Mössbauer effect methods. As it will be shown the variation of the saturation magnetic moment per molecule with the sample composition can be explained on the basis of the collinear magnetic moment ordering model and the elaborated and experimentally verified cation distribution model.

## 2. Experimental Methods and Results

The samples were prepared by the usual sintering process using oxides as the starting materials. The homogeneity of the samples was proved by the X-ray diffraction method.

X-ray diffraction studies were performed at room temperature with a DRON-1 type diffractometer using CuK$\alpha$ radiation. The values of the lattice constant $a_0$ have been derived for the $t = 0.0, 0.2, 0.4, 0.63, 0.75, 1.0, 1.25, 1.35, 1.5, 1.75, 1.9, 2.0$ samples from the X-ray powder patterns. They are shown in Fig. 1.

Neutron diffraction investigations were performed with a neutron beam of 1.124 Å wavelength. The KSN type spectrometer [7] installed at the RA reactor in the Boris Kidrič Institute in Vinča was used. Measurements were carried out for the $t = 0.75$, 1.0, 1.25, 1.5, 2.0 samples at room temperature and for the $t = 1.25$, 1.5 samples at liquid nitrogen temperature. The (200) reflection predicted by the non-collinear spin ordering model was not observed (Fig. 2). The neutron diffraction spectra were analysed by a least-squares computer program. From their nuclear components the oxygen parameter (Fig. 3) and the cation distributions between the A- and B-sites (Fig. 4) were derived and compared with those calculated from the elaborated model [1]. From the magnetic components of the spectra, values of the magnetic moments of iron and nickel were derived. Values of the magnetic form factors for $Fe^{3+}$ and $Ni^{2+}$ used in the calculations were taken from [11] and [12], respectively. The obtained results are shown in Fig. 5.

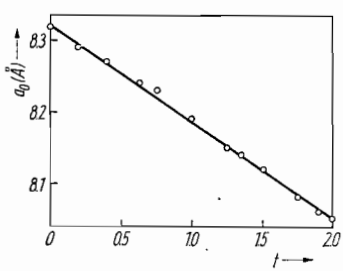


Fig. 1. Variation of the lattice constant $a_0$ with composition $t$

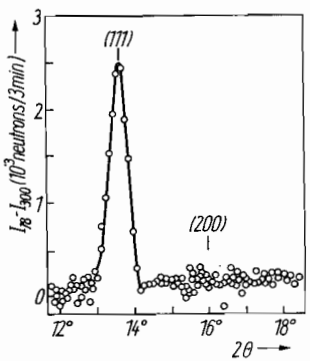


Fig. 2. Difference in neutron intensities measured at 78 and 300 K for the slowly cooled $t = 1.5$ sample

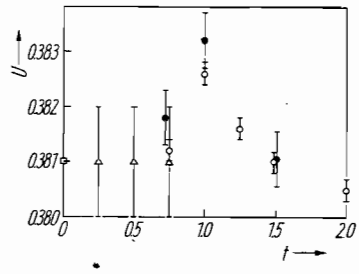


Fig. 3. Variation of the oxygen parameter $u$ with sample composition $t$. ○ this work, ● [6], □ [8], △ [9]

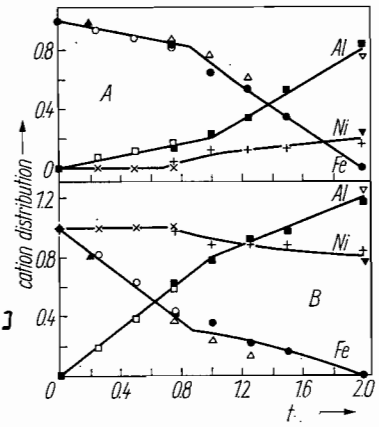


Fig. 4. Cation distributions in nickel ferrite-aluminates. ●, ■, + neutron diffraction data (this work); △ Mössbauer effect data (this work); ▲ Mössbauer effect data [4]; ○, □, × X-ray diffraction data [9]; ▽, ▼ X-ray diffraction data [10]

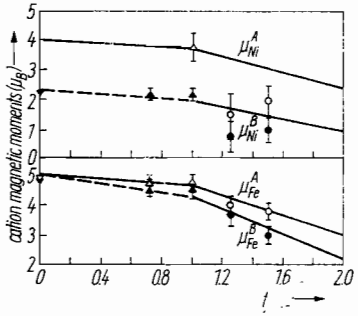


Fig. 5. Variation of the cation magnetic moments measured at liquid nitrogen temperature with sample composition $t$. ○, ● this work; △, ▲ [6]; ▽, ▼ room temperature data [13]

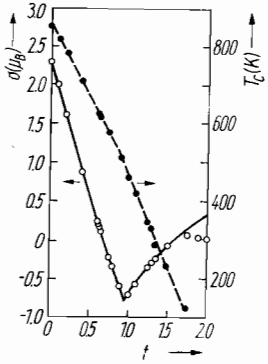


Fig. 6. Variation of the saturation magnetic moment per molecule $\sigma$ (○) measured at 78 K and the Curie temperature $T_C$ (●) with chemical composition $t$

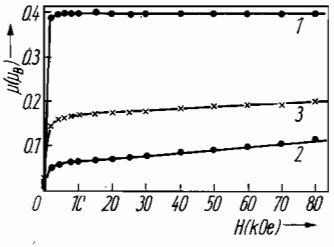


Fig. 7. Magnetization isotherms measured at 78 K in strong magnetic fields. (1) Slowly cooled $t = 1.25$ sample, (2) slowly cooled $t = 1.5$ sample, (3) $t = 1.5$ sample quenched from 1473 K

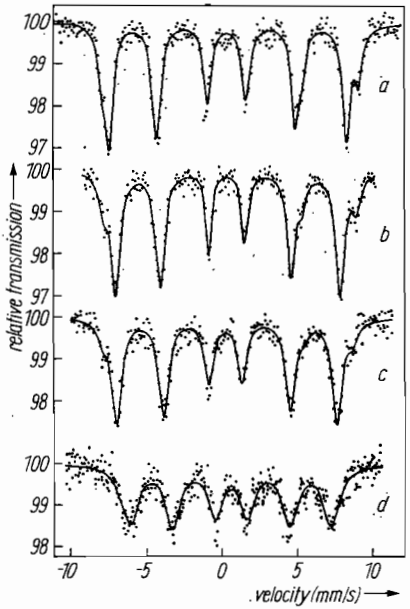


Fig. 8. Mössbauer absorption spectra measured at 78 K for the (a) $t = 0.75$, (b) 1.0, (c) 1.25, and (d) 1.5 samples

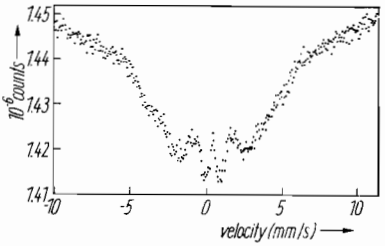


Fig. 9. Mössbauer absorption spectrum measured at 295 K for the $t = 1.25$ sample

Magnetometric measurements were performed for 20 samples with different $t$ over the temperature range 78 to 900 K and in magnetic fields up to 10 kOe [5]. A modified magnetic balance of Sucksmith's type was used [14]. Measurements of the magnetization as a function of the magnetic field intensity and temperature allowed the determination of the saturation magnetic moments per molecule at 78 K and Curie temperatures (Fig. 6). For the slowly cooled $t = 1.25$, 1.5 samples and for the $t = 1.5$ sample quenched from 1473 K additional isotherms were determined at 78 K in magnetic fields up to 80 kOe (Fig. 7).

Mössbauer absorption spectra were taken at room and liquid nitrogen temperatures for the non-enriched samples with $t = 0.75$, 1.0, 1.25, and 1.5. A $^{57}$Co(Cr) source and a constant acceleration spectrometer with optical velocity calibration were used. The absorption spectra were analysed with a least-squares computer program. Values of the internal magnetic fields, isomer shifts and quadrupole splittings as well as distributions of iron ions were determined for the octahedral and tetrahedral sublattices. Some of the absorption spectra are shown in Fig. 8 and 9.

## 3. Discussion of the Results

X-ray, neutron diffraction, and Mössbauer effect data may be explained by the equilibrium cation distribution model recently elaborated for nickel ferrite-aluminates. According to it, for $t$-values varying from zero to about 0.9 the aluminium cations replace the iron cations in A- and B-sites linearly with the probability ratio 1:4. There is no exchange of nickel cations between the A- and B-sites. For $t$-values varying from 0.9 to 2.0 the aluminium cations are embedded in the A- and B-sites linearly with the probability ratio of about 3:2. The corresponding ratio for the replacement of the iron cations is slightly higher than 3:2 due to the replacement of the nickel cations from B-sites in A-sites. There is a remarkable difference in the above-mentioned ratios at the $t$-value of about 0.9. This should imply a discontinuity of the crystal properties. It is assumed that beyond the discontinuity region the crystal parameters are varying

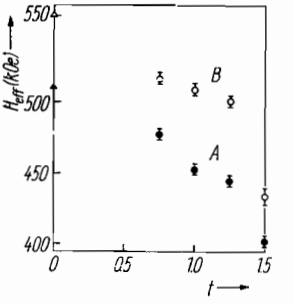


Fig. 10. Variation of the effective magnetic fields measured at 78 K acting on $^{57}$Fe nuclei with chemical composition $t$. ○, ● this work; △, ▲ NMR data [15]

smoothly and match the parameters of nickel ferrite at $t = 0.0$ and the parameters of nickel aluminate at $t = 2.0$.

The lattice constant (Fig. 1) decreases with increasing aluminium content due to the replacement of the iron cations by the smaller aluminium ones. This variation is found to be nearly linear in accordance with Vegard's law. However, the discontinuity of the oxygen parameter at a $t$-value of about 0.9, predicted by the cation distribution model, is clearly seen (Fig. 3). In order to get some more information concerning this effect precise measurements of crystal parameters should be performed in a narrow region of $t$ near 0.9.

The cation distributions derived from the neutron diffraction patterns are in good agreement with those predicted by the discussed model (Fig. 4).

The oxygen parameter and the lattice constant are larger for samples quenched from 1473 K than for the slowly cooled ones.

As the aluminium content increases in nickel ferrite-aluminates the magnetic coupling is weakened from that of nickel ferrite at $t = 0.0$ to that of paramagnetic nickel aluminate at $t = 2.0$. This can be clearly seen from the decrease of the Curie temperature (Fig. 6), the magnetic moments of iron and nickel ions measured at 78 K (Fig. 5), as well as the effective magnetic fields acting on $^{57}$Fe nuclei (Fig. 10). The decrease in Curie temperature with increasing aluminium content is found to be nearly linear. However, this decrease is a little faster for samples with $t > 1$. The reduction of the magnetic moments of iron and nickel ions is also higher for samples with greater $t$-values, and for a given $t$-value is more pronounced at the B-sites. All these dependences are due to the distribution of iron, nickel, and aluminium ions between the A- and B-sublattices. Due to the covalence effects the internal magnetic fields acting on $^{57}$Fe nuclei are smaller in the A-sites as compared with those in the B-sites.

Early Mössbauer investigations [4] were performed at room and liquid nitrogen temperatures for the $^{57}$Fe enriched samples with $t = 0.2$, 0.5, 1.0, 1.4, 1.6, and 1.8. Two Zeeman patterns were attributed both to the $t = 0.2$ and 0.5 samples, four ones to the $t = 1.0$ sample, and three ones to each of the $t = 1.4$, 1.6, 1.8 samples. Results for the samples with $t \geqq 1$ were interpreted as evidence of the non-collinear spin ordering in the A-sublattice. Our Mössbauer absorption spectra do not confirm this assumption. They are easily interpreted as being due to two six-line hyperfine patterns corresponding to $^{57}$Fe in A- and B-positions. The influence of random distributions of nickel and aluminium ions around iron ions on the internal magnetic fields manifests itself as the broadening of Zeeman components of the absorption spectra measured at room temperature for the $t = 0.75$, 1.0 samples. The hyperfine structure of the absorption spectrum observed at room temperature for the $t = 1.25$ sample (Fig. 9) is not resolved. This spectrum seems to be caused by superparamagnetic relaxation effects. The $t = 1.5$ sample is paramagnetic at room temperature and its absorption spectrum shows only quadrupole splitting with $\Delta E_q = (0.63 \pm 0.03)$ mm/s.

The results of magnetization measurements proved the collinear ordering of atomic spins for the samples with $t$ up to 1.25. Magnetic saturation of these samples was obtained in fields of about 4 kOe. However, for the $t = 1.5$ samples, both slowly cooled and quenched from 1473 K, no saturation of the magnetization at 78 K was obtained even in fields up to 80 kOe. Similar, but steeper, magnetization isotherms were reported for $MnCr_2O_4$ and $MnFe_2O_4$ spinels [16] for which the neutron diffraction studies revealed non-collinear spin ordering. The presence of such ordering in spinels should be evidenced as an additional (200) reflection in the neutron diffraction patterns. The lack of such a reflection for the $t = 1.5$ sample (Fig. 2) seems to rule out this possibility. On the other hand, as it was suggested in [17], the lack of saturation of the magnetization of $BaFe_9O_{12}$ in strong magnetic fields can be attributed to a statistic angular magnetic structure which, however, cannot be observed by a neutron diffraction method [18]. In our opinion the slight increase in the magnetization of the $t = 1.5$ sample in high magnetic fields seems to be evidence of the superparamagnetic behaviour of this sample.

The change of the spin ordering from collinear to non-collinear should have a strong influence on the variation of the saturation magnetic moment per molecule with chemical composition. The value of the saturation magnetic moment per molecule measured at 78 K decreases almost linearly with increasing $t$ from $2.3\mu_B$ at $t = 0.0$, approaches zero at $t = 0.63$, and reaches the minimum $-0.72\mu_B$ at $t$ equal about 1.0, beyond which an increase is observed (Fig. 6). Negative values are the result of the predominance of the magnetization of the A-sublattice over that of the B-sublattice. To explain the variation of the saturation magnetic moment per molecule with chemical composition collinear spin ordering was assumed. The explanation is based on the cation distribution model for nickel ferrite-aluminates and a slow decrease in iron and nickel magnetic moments measured at 78 K with an increase in $t$. The best fit to the measured values (solid line in Fig. 6) was obtained with the cation distributions previously reported [1] and with the values of iron and nickel magnetic moments shown by solid lines in Fig. 5. The values 0.809 and 1.191 for the distribution of aluminium ions in the A- and B-sites in nickel aluminate were taken in the cation distribution calculations. They are in good agreement with the average values of those determined with X-ray [10] and neutron diffraction [1] methods. Values of the iron and nickel magnetic moments obtained from the computer fit are compared with those derived from neutron diffraction patterns. Apart from the values of nickel magnetic moments in the A-site for the 1.25, 1.5 samples, satisfactory agreement is obtained between the values derived from neutron diffraction and from magnetometric investigations. Large errors for the values of nickel magnetic moments in the A-sites are due to the small amount of nickel in these positions and to the fact that neutron nuclear scattering amplitudes for nickel and iron are very close to each other. The discrepancy between the measured values of saturation magnetic moments per molecule and the fitted curve for the samples with $t > 1.5$ is most probably due to the diminution of the magnetic coupling and relaxation processes.

From the temperature dependence of magnetic susceptibility of nickel aluminate the value of the Curie constant 1.041 $mol^{-1}$ and the effective magnetic moment $2.9\mu_B$ were derived.

The influence of random distributions of nickel and aluminium cations around iron cations on the effective magnetic fields as well as superparamagnetic processes are very attractive phenomena for further Mössbauer investigations which are in progress.

## References

[1] J. J. BARA, ~~to be published.~~ phys. stat. sol., (a) 44, 737 (1977)
[2] L. R. MAXWELL and S. J. PICKART, Phys. Rev. 92, 1120 (1953).

[3] J. S. Smart, Phys. Rev. **94**, 847 (1954).
[4] V. F. Belov, M. N. Shipko, T. A. Khimich, V. V. Korovushkin, and L. N. Korablin, Fiz. tverd. Tela **13**, 2018 (1971).
[5] L. Kozłowski and W. Zarek, Acta phys. Polon. **A42**, 663 (1972); **A43**, 79 (1973).
[6] S. Nizioł, phys. stat. sol. (a) **17**, 555 (1973).
[7] S. Krašnicki, J. Pawełczyk, and H. Rapacki, Nukleonika (Warszawa) **7**, 223 (1962).
[8] J. M. Hastings and L. M. Corliss, Rev. mod. Phys. **25**, 114 (1953).
[9] N. M. Chedotaev, A. G. Zalazinskii, V. F. Balakirev, M. T. Kushko, V. M. Bich, G. P. Popov, and G. I. Chufarov, Izv. vuzov (Ivanovo), Khim. i khim. Tekhnol. **19**, 516 (1976).
[10] F. C. Romeijn, Philips Res. Rep. **8**, 321 (1953).
[11] A. J. Freeman and R. E. Watson, Phys. Rev. **118**, 1168 (1960).
[12] D. E. Cox and V. J. Minkiewicz, Phys. Rev. B **4**, 2209 (1971).
[13] S. I. Youssef, M. G. Natera, R. J. Begum, B. S. Srinivasan, and N. S. Satya Murthy, J. Phys. Chem. Solids **30**, 1941 (1969).
[14] Z. Obuszko, Acta phys. Polon. **24**, 135 (1963).
[15] H. Abe, M. Matsuura, H. Yasuoka, A. Hirai, T. Hashi, and T. Fukuyama, J. Phys. Soc. Japan **18**, 1400 (1963).
[16] J. S. Jacobs, J. Phys. Chem. Solids **15**, 54 (1960).
[17] N. Jefimov and J. A. Mamały, Proc. Magnetic Conf. Moscow **3**, 55 (1973).
[18] K. P. Belov, Ferrites in Strong Magnetic Fields, Izd. Nauka, Moscow 1972.

*(Received July 7, 1977)*